Observation of transition radiation from relativistic heavy nuclei

Simon P. Swordy,* John Grunsfeld,*† Jacques L'Heureux, Peter Meyer,* Dietrich Müller,* and Kwok-Kwong Tang
Enrico Fermi Institute, University of Chicago, 933 East 56th Street, Chicago, Illinois 60637
(Received 23 March 1990)

We have made the first observation of transition radiation produced by relativistic heavy nuclei. The instrument used in this work is a large cosmic-ray detector for the space shuttle designed to measure the energy spectra of heavy nuclei in the cosmic radiation at TeV/nucleon energies. The response of the detector scales with the charge Z of the primary nucleus as expected from theory. The relative fluctuations in detected transition radiation from heavy nuclei are much smaller than those from singly charged particles, because of the large number of photons produced. This makes possible an accurate determination of the energy of the nucleus in the TeV/nucleon region by measurement of the transition radiation yield. The response of such a detector can be well extrapolated from accelerator measurements with singly charged particles.

I. INTRODUCTION

Transition radiation is generated if a charged particle crosses a boundary between media of different dielectric constants. The effect is a consequence of sudden changes in the electric polarization caused by the particle in the surrounding medium. We refer to the literature for a detailed mathematical discussion of this phenomenon.[1-3] However, some qualitative features of production and detection will be given here as an aid to the understanding of the results presented.

Measurements of transition radiation have been mostly performed in the x-ray region of the electromagnetic spectrum, since this is the region where, for highly relativistic particles, most of the radiated energy is emitted, and where individual quanta may be detected with high efficiency.[4-6] Typically, measurements are made with particles with Lorentz factors >1000. In the following we report, for the first time, the emission of x-ray transition radiation from highly relativistic *heavy nuclei,* and the utilization of this effect for the measurement of cosmic-ray energy spectra. This application of the effect depends on the expectation that the yield of radiation increases as Z^2 (where Z is the atomic number of the nucleus). Thus, contrary to singly charged particles with a very small number of photons, we may detect hundreds of transition radiation photons in each event, and the statistical fluctuations should be small enough to permit an accurate measurement of the energy of the incident nucleus from the transition radiation intensity. The mean transition radiation yield per Z^2 is expected to depend only on the speed of the particle. Thus we can actually determine the particle Lorentz factor $\gamma=E/mc^2$ [$\gamma=1/\sqrt{(1-\beta^2)}$, $\beta=v/c$, $E=$ particle energy, $m=$ particle mass, $c=$ speed of light]. For heavy nuclei this is the energy per unit atomic mass. Our measurements show that these expectations are well justified.

This work was performed with an instrument on the Spacelab-2 mission of the space shuttle Challenger in 1985.[7] The instrument is designed to measure the fluxes of galactic cosmic-ray nuclei heavier than lithium, up to Lorentz factors $\gamma\approx10^4$. An iron nucleus with $\gamma=10^4$ has a total energy $\approx6\times10^{14}$ eV, close to the region where a conspicuous steepening in the cosmic-ray spectrum has been observed.[8] The application of a transition radiation detector for this measurement is particularly attractive, as it permits the construction of large-area detectors with much lower mass than any other technique (for instance, hadronic calorimetry). However, the calibration of the energy response of the detector must be performed with singly charged particles since no terrestrial source exists for heavy nuclei at these energies. We must make sure that the expected scaling of the signal with Z^2 indeed holds, and that the magnitude of the fluctuations can be accurately predicted. This will be discussed in the following. We shall describe calibrations performed at Fermilab. We then discuss the observation of transition radiation from heavy nuclei in the cosmic radiation by the space experiment. We finally discuss the accuracy of this technique for estimating the energy of a nucleus, and compare the expected and calculated transition radiation response and fluctuations with observations.

II. TRANSITION-RADIATION DETECTION

A. Design principles

A typical transition radiation detector consists of a combination of a radiator in which, upon traversal of a relativistic particle, transition x-rays are generated, and a detector for these x-rays. Schematically, such a configuration is shown as an inset in Fig. 1. To enhance the efficiency and redundancy of transition radiation detection in practical applications, multiple layers of radiators and detectors are often employed. The transition x-rays are emitted, within a cone of half-angle $1/\gamma$ in the direction of motion of the particle. Therefore, particle and x-rays traverse the detector simultaneously and produce signals that, in general, cannot be separated in space or time. These features significantly constrain the design of an efficient radiator-detector combination. First, the radiator must consist of low-Z materials, such that x-rays

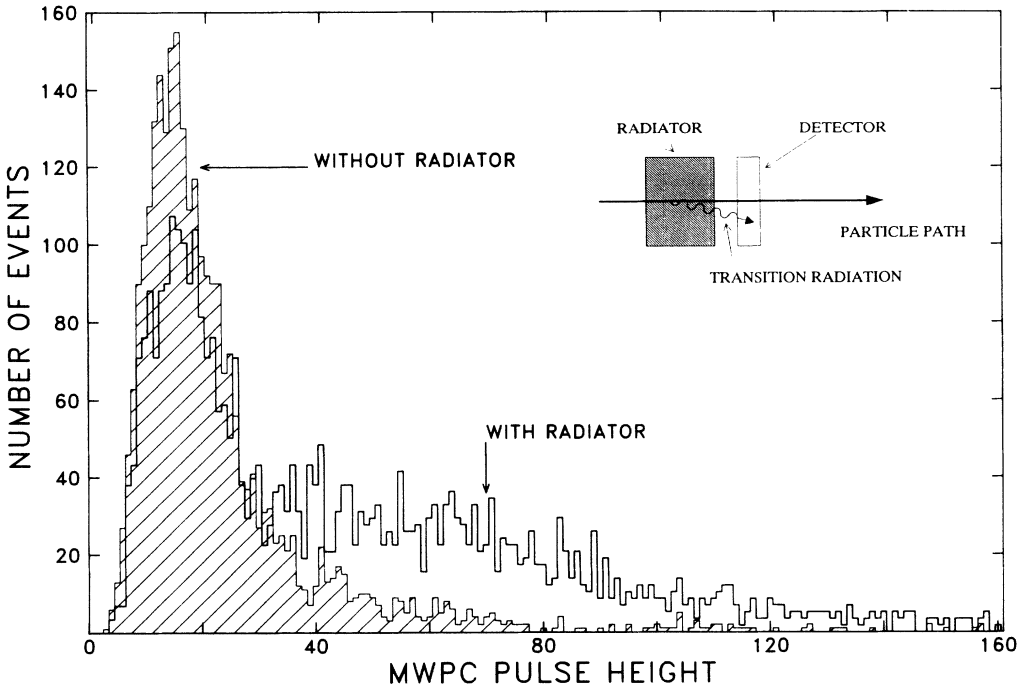

FIG. 1. The pulse-height distribution observed from a single multiwire proportional chamber in the transition detector for muons at 400 GeV/c. This includes the transition-radiation and ionization-loss components of the signal. The shaded distribution was obtained by replacing the radiator with an equivalent thickness of solid material, this gives only the ionization loss component of the signal. The inset shows the schematic arrangement of the detector.

are not reabsorbed within the radiator. Second, the detector must be an efficient absorber of x-rays but must, at the same time, be of low mass density to minimize the signal due to the ionization loss of the primary particle. One usually employs gaseous detectors, for instance, xenon-filled multiwire proportional chambers which are highly efficient for x-rays up to ≈ 40 keV.

The specific choice for a radiator-detector configuration depends on the desired application of the device, and requires careful optimization of a number of parameters. Detailed discussions are given in the literature;[6,10] and the following is just a brief summary of relevant facts.

First, the radiation yield of a *singly* charged particle at a single interface is small, of the order $\frac{1}{137}$ photons. Therefore, a radiator must contain several hundred interfaces if the radiation is to be efficiently detected. For particles with higher charge Z, one expects the yield to increase proportional to Z^2. To verify this Z^2 scaling is an objective of the present study. In many applications, a radiator is chosen that consists of multiple layers of low-Z material of thickness l_1 (plastic foils such as Mylar or polyethylene are easiest to use), with regular spacings l_2 of air between the layers. The radiation yield from such a configuration can be accurately calculated. It depends on the parameters l_1 and l_2, and the plasma frequencies ω_1 and ω_2 of foil and gap material, respectively, and on the Lorentz factor γ of the particle. Most important for practical applications is the γ dependence of the radiation yield. The radiation exceeds the detection threshold only if the Lorentz factor is rather large. The intensity then increases with γ, initially proportional to γ, but reaches saturation, typically around $\gamma \approx (\omega_1/c)/\sqrt{l_1 l_2}$. The radiation extends over a range of x-ray frequencies and becomes harder with increasing γ. When saturation is reached the maximum intensity is emitted around a frequency of $\omega_m = l_1 \omega_1^2 / 2\pi c$.

For our application we wish to use a transition radiation detector with large dynamic range: the threshold of the instrument should be at a relatively low Lorentz factor of a few hundred, but saturation should not be reached until values around $\gamma \approx 10^4$. The latter requirement calls for radiators with relatively large foil thickness l_1 and large spacing l_2. It also leads to the emission of fairly hard x-rays. However, such a radiator is not very desirable for low γ values as the softer x-rays produced in this case would tend to be reabsorbed in the radiator. To obtain good response at low γ (i.e., a low threshold of detection), a radiator with small values of l_1 should be chosen. These considerations make the choice of a "graded" radiator attractive: a combination of a "thick foil" radiator, with hard, penetrating x rays and large saturation value, followed by a "thin foil" radiator with softer x-ray emission but better performance at low γ

TABLE I. (a) Transition-radiation-detector composition and (b) fiber dimensions.

(a)

	Composition	Effective thickness (g/cm^2)
Radiator 1	15.2 cm of thick fibers	≈ 0.61
	6.7 cm of thin fibers	≈ 0.31
Radiators 2–6	5.0 cm of thick fibers	≈ 0.20
	6.7 cm of thin fibers	≈ 0.31
Detectors 1–6	2 cm MWPC's filled with 25% Xe, 15% CH_4, 60% He	

(b)

	Diameter (μm)	Mean spacing (μm)	Effective diameter (μm)[a]
Thick fibers	17	380	21
Thin fibers	2–5[b]	100	4.5

[a]The effective diameter given for the fibers is the mean separation between interfaces along one axis, assuming the orientation of the fibers to be isotropic. This corresponds to the foil thickness of an equivalent parallel foil radiator.
[b]The thin fibers have a range of thicknesses.

values.

Finally, it is important to realize that regular foil radiators can be replaced by irregular structures such as foams or fibers.[11,21] In many cases, the radiation yield of such substances equals that of foil radiators of the same average thicknesses. The use of such materials considerably simplifies the mechanical construction of the detector system.

In the present work we have used battings of polyolefin plastic fibers as a radiator. These are rather transparent to x rays, and can be implemented in large area (several m^2) detectors more easily than multiple layers of stretched foils. We use two sizes of polyolefin fibers: "thick" fibers with a diameter of 17 μm and "thin" fibers with a range of diameters between 2 and 5 μm. Each radiator has a section of thick fibers upstream, which is followed by layers of thin fibers. As mentioned, such a combination is expected to extend the range of Lorentz factors over which the detector system can be used. This expectation has been verified in previous accelerator tests.[11] The entire transition radiation detector system used in our experiment consists of six radiator-detector layers. The details of the system are summarized in Table I. Note that radiator 1, the most upstream radiator, has a larger layer of thick fibers than the following radiators.

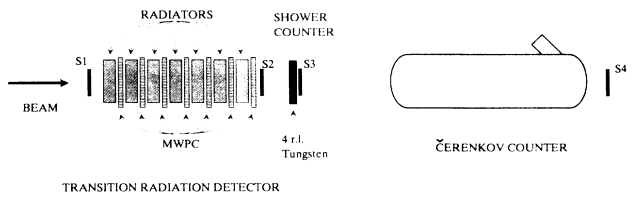

FIG. 2. Schematic of the experimental arrangement at Fermilab. The transition-radiation detector consists of six radiator–multiwire-proportional-chamber pairs. This experiment was used to determine the response of the detector for singly charged particles.

This is done to utilize the effect of "x-ray feedthrough" which will be discussed below.

B. Accelerator measurements

We have combined the radiators described above with xenon filled multiwire proportional chambers (MWPC's) and have performed measurements with singly charged particles at an accelerator beam. First measurements with electrons have been reported previously.[11] Here we shall present results from an exposure to protons, pions, and muons. These measurements were made in Lab C of the neutrino beam line of Fermilab.

The experimental arrangement is shown in Fig. 2. Two scintillators S1 and S2 are used to trigger data collection. A shower counter consisting of 4 radiation lengths of tungsten followed by a plastic scintillator is placed downstream to reject the small contamination of electrons which is $<1\%$. For particle identification, a 61-m-long gas Čerenkov counter downstream is used. This counter can be filled with either nitrogen or helium to vary the threshold. Since there was an intervening sequence of magnets between the Čerenkov counter and the transition radiation detector, a beam defining scintillator S4 was placed just downstream of the counter to identify particles which passes through the Čerenkov counter but produced no signal. The beam momentum was known to better than 1%.

The transition radiation detector (TRD) has six radiator-MWPC combinations and a total thickness of ≈ 5 g/cm^2 of plastic material. The MWPC's have a smaller area but are otherwise identical to those used in the space experiment. Each has 50-μm-diameter stainless-steel wires spaced at 1-cm intervals. The windows are 50-μm-thick aluminized Mylar, with 2-cm spacing between the windows. In each MWPC, wires are connected in groups of five to charge amplifiers. The beam is centered on the middle of three groups, and the signal is measured from the central group. The two side groups are used to reject particles outside of the main beam

which is a few cm in diameter. The radiators can be removed from the apparatus and replaced by equivalent thicknesses of solid plastic to study the particle ionization loss component of the detector signal. The MWPC's and radiators can be inclined up to 60 deg with respect to the beam line, in order to study the variations of response with angle of the particle path to the detector planes. The MWPC's were purged with a gas mixture of 25% xenon, 15% methane, and 60% helium. Both of these additives were chosen for their low stopping power relative to xenon. Previous experiments[11] had shown that this mixture optimizes the ratio of transition radiation signal to ionization loss for the radiator chosen. The gains of the MWPC's remained stable to $\approx 1\%$ for an individual run and within 10% over the whole period of these tests. The chamber gain at the operating voltage of 2.1 kV is $\approx 10^4$.

The signals from all counters, including the scintillators and the Čerenkov counter, were fed to a multiple-input 12-bit analog-to-digital converter (ADC) computer system which recorded events onto magnetic tape for later analysis. For most runs the particle beam contained mainly protons and pions with some small admixture of kaons and leptons. One set of data was taken at 400 GeV/c with a deep absorber upstream of the apparatus and of the momentum defining magnet. This ensured that only muons could reach the counters. For the other runs, pions were discriminated from protons at each beam momentum by setting the gas Čerenkov counter threshold at the appropriate level. Particles that produced a single particle signal in S4 but did not pulse C1 were deemed to be protons. Those that gave an appropriate signal in C1 were pions.

C. Results

The TRD response was measured over a range $55 < \gamma < 3800$. A typical pulse-height spectrum at $\gamma = 3800$ from a single MWPC is shown in Fig. 1. Plotted are the particle ionization loss distributions produced when the radiators are replaced with an equivalent thickness of solid material, and the distribution with radiators in position. Clearly, in around two-thirds of the events the transition radiation adds at least one photon to the MWPC signal, and the mean photon energy is comparable to the mean ionization loss of the particle in the chamber, around 5 keV.

We wish to know how the mean energy deposited in the chamber varies with γ, including the transition radiation and the ionization loss. This is shown in Fig. 3 for particles at normal incidence to the six MWPC's. With the radiators in position, the transition radiation component begins to appear at $\gamma \approx 450$ and then rises as γ increases. This signal does not saturate over the range of these measurements. Such a response is well suited to an application such as ours where a measurement of γ over a wide range is desired. Also plotted are the measurements of the mean ionization loss component of the signal with the radiators replaced with an equivalent thickness of solid material. Figure 3 illustrates that the relativistic rise in energy deposited by ionization loss is still discernible in this gas up to $\gamma \approx 4000$. Other authors have indicated that xenon, providing the dominant stopping power in our mixture, should indeed exhibit a large relativistic rise.[12]

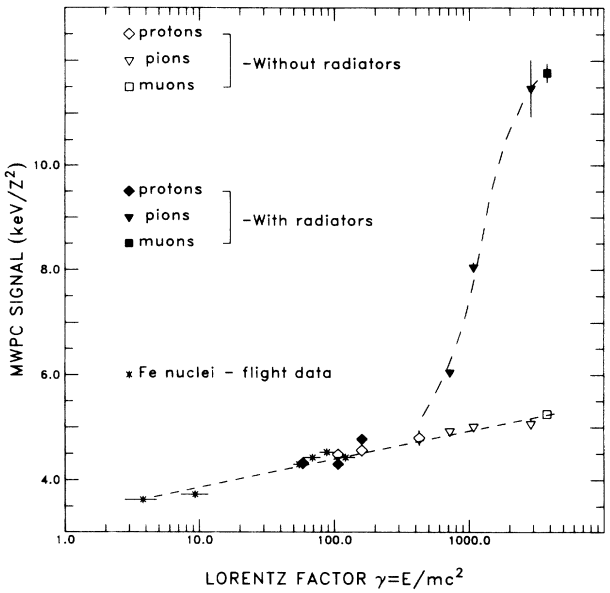

FIG. 3. The response of the transition-radiation detector for normally incident particles (filled symbols). The open symbols indicate the ionization loss component of the signal. The iron nuclei data were collected with the cosmic ray instrument described in the text.

Figure 4 gives the response as the detector is inclined relative to the particle beam. This is important for measurements of the isotropic cosmic-ray flux, which will cover a large range of incident angles. For a particle in-

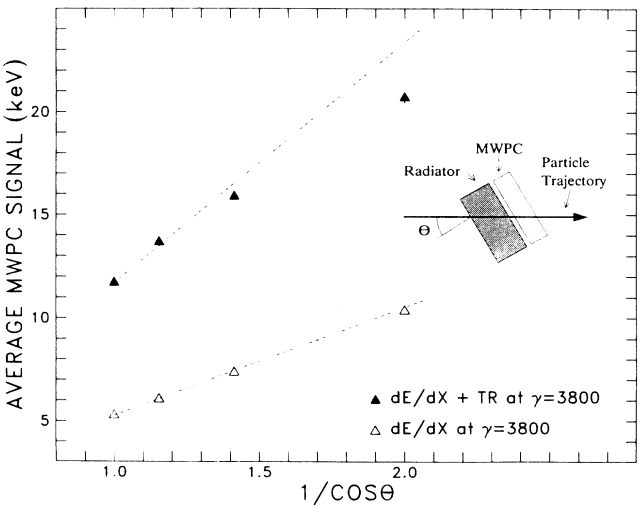

FIG. 4. The variation of the transition-radiation-detector response with incoming particle angle. At large angles the transition radiation component of the signal (upper points) begins to deviate from proportionality to $1/\cos\theta$ (upper dashed line). The ionization-loss signal, however, is strictly proportional to $1/\cos\theta$ (lower points).

cident at an angle θ to the vertical, both the effective thickness of the radiator and that of the detector, will be increased by a factor $1/\cos\theta$. The increase in radiator thickness will lead to an enhancement in the number of transition radiation photons produced. However, this enhancement may be less than proportional to the thickness increase due to reabsorption in the radiator. The greater thickness of the detector will, on the other hand, enhance the detection probability for x rays. The combined effect leads one to expect an increase in the detected signal with increasing angle θ. The magnitude of the effect depends on the dimensions and materials of radiator and detector. As Fig. 4 indicates, for our case the increase is nearly proportional to $1/\cos\theta$ up to $\theta \approx 45°$, but falls below this proportionality for larger angles. The ionization loss signal in the detector, which is superimposed upon the transition radiation signal, will however scale strictly with $1/\cos\theta$ as it is proportional to the amount of material along the particle path. This behavior is also shown in Fig. 4.

Another effect important for practical applications is the "feedthrough" of transition radiation photons through a stack of radiators and detectors. It is possible that an x-ray photon is not detected in the MWPC directly behind a radiator, and that it penetrates the following material until it is absorbed in one of the downstream MWPC's. As the transition radiation spectrum hardens with increasing Lorentz factor of the particle,[10] this effect is most pronounced for the more energetic particles. Figure 5 shows evidence for this effect, an increase in the transition radiation signal with each chamber in the beam direction, for particles with $\gamma = 3800$. However, the effect is quite small as our radiator stack was purposely designed to provide a nearly uniform response for all MWPC's by making the first radiator significantly thicker than the following (see Table I).

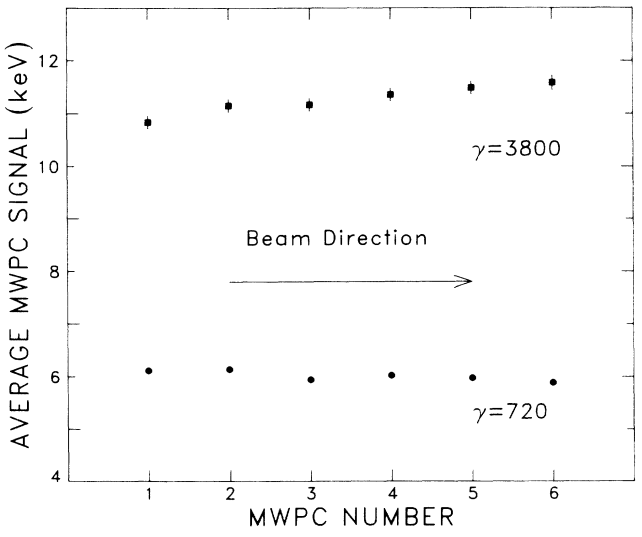

FIG. 5. The mean transition-radiation-detector signal from each multiwire proportional chamber in the beam direction. (The most upstream chamber is number 1.) The upper points, taken at high Lorentz factor, show the increase in signal with depth in the detector. The lower points, at lower Lorentz factor, show constant response.

The effective use of a TRD assembly such as this is critically dependent on the extent of the fluctuations of the observed signals, which are large for singly charged particles as illustrated in Fig. 1. Even if multiple measurements are made, the remaining fluctuations in the signals from *singly charged particles,* as typically encountered in accelerator experiments, permit at most a gross estimate of γ. However, for more highly charged particles, such as the relativistic nuclei found in the primary cosmic rays, the signal fluctuations are considerably reduced and a far more accurate determination of γ is possible with a small number of radiator-MWPC pairs. This will be discussed further in Sec. IV.

III. THE COSMIC-RAY EXPERIMENT

Our cosmic-ray detector is shown in Fig. 6. This instrument was designed to measure the fluxes of cosmic-ray nuclei heavier than lithium above $\gamma = 40$. It was flown on the Spacelab-2 mission of the space shuttle in 1985.[13] Two plastic scintillation counters are used to trigger the instrument to select downward moving particles and to measure the particle charge. The TRD consists of six radiator-MWPC pairs. The MWPC's are segmented in 5-cm-wide groups of wires, each of which is pulse-height analyzed. This serves as a hodoscope to determine particle trajectories, as well as measuring the transition radiation yield. The spherical end caps of the detector are used as integrating gas Čerenkov counters. The inner surfaces are painted with a high reflectance white paint, and 48 photomultipliers are used for each counter. The threshold of these counters is set at $\gamma = 40$. Because of the extremely low flux of cosmic-ray nuclei at high energies, this instrument was designed to be as large as possible within the constraints of the space-shuttle

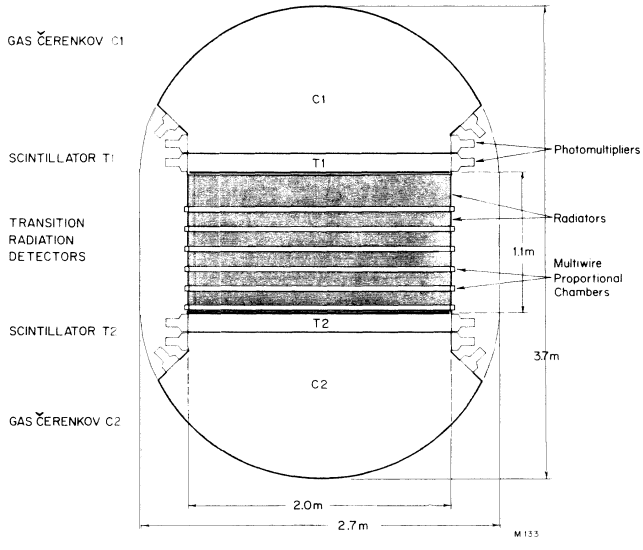

FIG. 6. Schematic cross section of the cosmic-ray instrument.

payload bay. The collecting aperture defined by the scintillation counters for an isotropic flux of particles is ≈ 5 m^{2}str. The detailed operation of the instrument is described elsewhere;[14] here we shall concentrate on the transition radiation measurement.

IV. OBSERVATION OF TRANSITION RADIATION FROM HEAVY NUCLEI

The flight data from the instrument shown in Fig. 6 were recorded on the ground onto magnetic tape for later analysis. Of the several million events collected, only a small fraction had high enough energy to be in the response region of the TRD, at $\gamma > 450$. An illustration of the flight data is shown in Fig. 7. Here, nuclei in the range $7 < Z < 30$ are selected on the basis of the pulse height measured with the scintillation counters, and the transition radiation and Čerenkov signals for individual events are displayed. The signals for each event have been normalized to vertical incidence and divided by Z^2 to provide the yield per unit pathlength normalized to unit charge. The only constraints applied to the data for this plot are that the scintillation counters identify the event as a nonfragmenting nucleus which moves downward, and that the signals from each of the two Čerenkov counters are consistent. The dominant elements in this data set are nuclei of oxygen, neon, magnesium, silicon, and iron. The Čerenkov emission rises sharply with energy above the threshold of $\gamma = 40$, and approaches a saturated yield level. The Čerenkov signal is blurred by photoelectron statistics and by a systematic background emission from the white paint layer which coats the walls of the volume (the mean background level, which is $\approx 15\%$ of the saturated yield, has been subtracted from these data). Indicated on the figure are energy calibrations of both the Čerenkov and transition radiation signals. For the transition radiation these are based on the accelerator data of Fig. 3. For the Čerenkov signal the response function has been calculated analytically and normalized to the saturated yield level at $\beta = 1$ determined from the data. Figure 7 clearly shows a small population of events with the Čerenkov counter in saturation, but with very large signals in the transition radiation detectors.

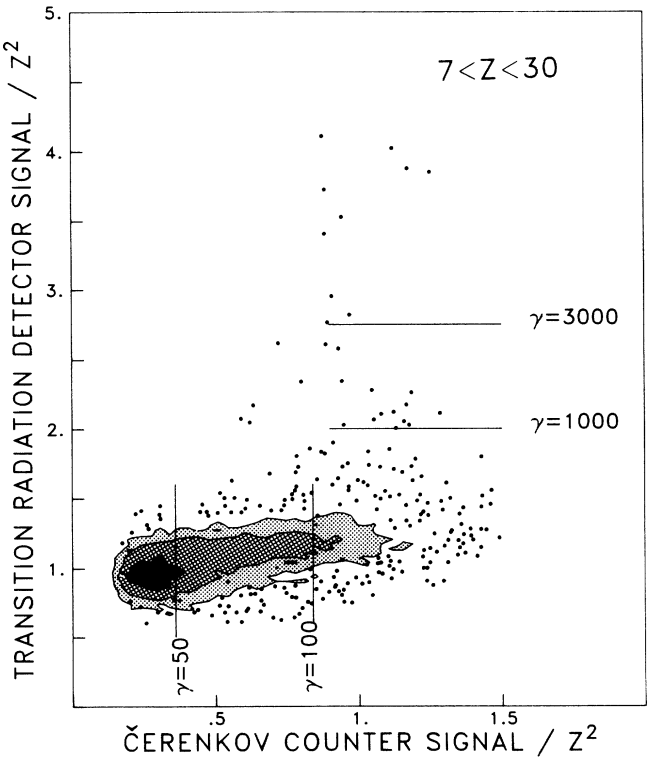

FIG. 7. Cosmic-ray nuclei event signals in the instrument for the range $7 < Z < 30$. For each event the transition radiation detector and Čerenkov signal divided by Z^2 are plotted. Examples of the energy calibrations are marked as lines for each counter. The contour levels are drawn where the event density is too large to distinguish individual points, each level represents a factor of 4 increase in event density. The area contained inside the lowest contour contains ≈ 9000 events. As expected, all the transition radiation events lie at the saturated level in the Čerenkov counter.

The high-energy nuclei events in Fig. 7 are sparse because of the low fluxes of cosmic rays at these energies. Even several days exposure of m^2 sized detector in space lead to only a few tens of heavy nuclei above $\gamma = 1000$, i.e., an energy of ≈ 1 TeV/nucleon. However, the observed data confirm excellently to the expected trend in the two energy measuring devices and, particularly at high γ, they are not obscured by surrounding background. The absence of events with large pulse heights in the TRD for the "low"-energy region of the Čerenkov counter demonstrates that there is no unexpected background and that the events with large pulse heights are clearly due to the production of transition radiation. Each TRD pulse height actually is the average signal from the six MWPC's. The large pulse heights are not dominated by the contribution from just one of the MWPC's: An examination of the signal distribution in the six MWPCs' shows that all detectors collect consistent transition radiation signals. The details of the fluctuations in these signals will be discussed below.

The nuclei above $\gamma = 3000$ have energies larger than several TeV/nucleon and deposit hundreds of x-ray photons in each MWPC. The saturation level for TRD could not be observed at the highest available accelerator energy. However, the data of Fig. 7 show an indication for the clustering of the largest signals which would imply a saturation of response around $\gamma \approx 7000$.

This is the first time that transition radiation in the x-ray region has been observed from heavy nuclei. In the following we shall discuss the expected yield variation and fluctuations, and compare these with our observations.

V. PROPERTIES OF TRANSITION RADIATION FROM NUCLEI

Detection of transition radiation x-rays is limited at low energy by reabsorption in the radiator, and a high-energy saturation is caused by interference between the

various interfaces of the radiator.[10] Previous studies of the spectrum of the transition radiation show a distribution with a broad maximum.[10] For the radiator properties of Table I this spectrum extends from a lower bound of ≈ 3 keV to about 15 keV. The spectrum drops rather rapidly at higher x-ray energies. That makes the measured signal distribution due to transition radiation x-rays quite different from the distribution of signals due to knock-on electrons from the primary particle, which has a long "tail" toward high energies.

The yield of transition radiation is expected to scale very closely at Z^2 (where Z is the charge of the particle). Studies of Čerenkov radiation, which has similarities to transition radiation, in that it arises from bulk polarization of the medium, have shown no significant deviation from this Z^2 scaling.[15] The particle ionization loss is also expected to scale with Z^2. We have investigated the Z dependence of the ionization loss signal in measurements at the LBL Bevelac accelerator.[16] The Z^2 scaling is confirmed by the cosmic-ray data from the present experiment: we have selected cosmic-ray nuclei in the range of response of the gas Čerenkov counter ($40 \leq \gamma \leq 150$), or in an energy interval around 10 GeV/amu where the geomagnetic field acts as a rigidity filter and therefore provides an energy measurement.[17] For these nuclei the transition radiation detector signals are due to ionization loss only and, as Fig. 3 shows for iron nuclei, are strictly proportional to Z^2 when compared to accelerator measurements with singly charged particles.

The resolution of a transition-radiation detector is determined by the extent of the fluctuations in the observed signals and by the number of individual detectors. Signal variations arise from the statistics of transition radiation and from fluctuations in the ionization loss signal of the charged particle. In fact, the latter are a major factor in determining the overall resolution. In the following we shall consider the extent of this "background" variation and then combine it with the transition radiation fluctuations to calculate the overall detector performance.

Normalized energy-loss distributions for oxygen and iron nuclei in a single MWPC, again selected for low energy, are shown in Fig. 8. Obviously, the relative probability of a fluctuation leading to a large pulse height is much smaller for the more highly charged nuclei than for singly charged particles (see Fig. 1). The measured relative rms width of the energy-loss distributions and the full width at half maximum (FWHM) as a function of charge for singly charged particles and for the more abundant heavier nuclei in the cosmic rays are shown in Fig. 9. The magnitudes of these widths agree well with results obtained in calibration measurements in the Bevalac accelerator.[16] The relative rms of all nuclei are consistent with the dashed curve shown which is a fit to the function

$$\Gamma_{\text{rms}}^2 = \frac{a_0^2}{Z^2} + a_1^2 ,$$

where Γ_{rms} is the relative rms width of the MWPC distribution, a_0 and a_1 are constants of the fit, a_1 representing the finite resolution of the MWPC. For this experiment

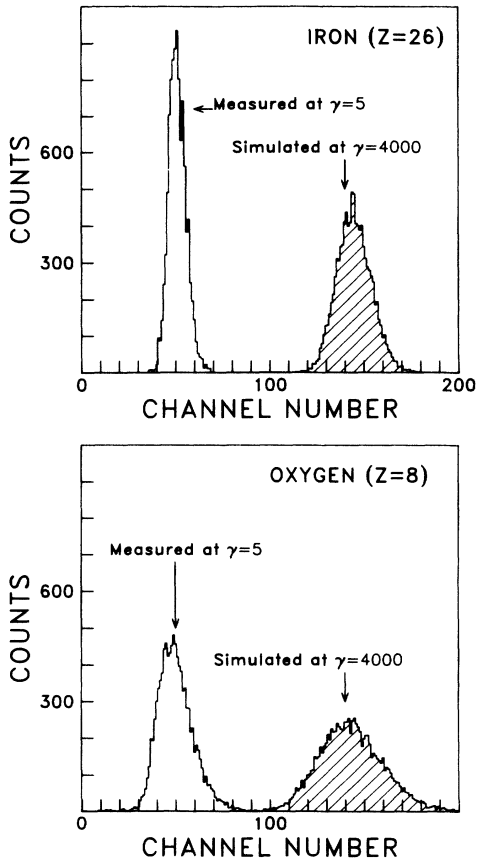

FIG. 8. Signal distributions in one multiwire proportional chamber of the transition-radiation detector for oxygen and iron nuclei. The unshaded distributions are measured cosmic-ray data at low energy, the shaded distributions are simulated for high-energy nuclei in a manner described in the text.

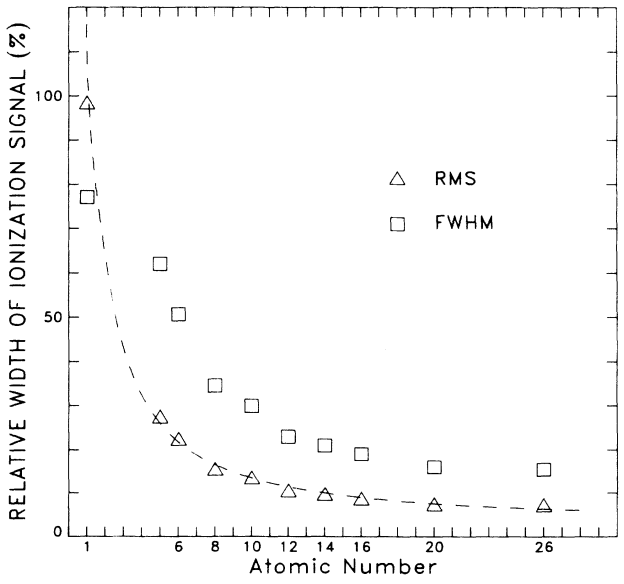

FIG. 9. The measured relative rms width (Γ_{rms}) and full width at half maximum (FWHM) of the ionization-loss signal distributions in one multiwire proportional chamber as a function of atomic number, Z. The curve is a fit to a function of the form $\Gamma_{\text{rms}}^2 = a_0^2/Z^2 + a_1^2$ for the rms width.

$a_1 \approx 0.04$ and $a_0 \approx 1.3$. For iron nuclei this results in a relative rms width of $\approx 7\%$, compared to $\approx 100\%$ for singly charged particles. The FWHM for singly charged particles is not well described by a similar function fit to the highly charged nuclei. The reason for this can be understood by considering that there is a qualitative difference in the energy-loss distribution observed in the MWPC's with either singly charged particles or with heavy nuclei. In the first case, the *maximum* possible energy transfer to an atomic electron is much larger than the average energy lost by the particle. The distribution then becomes asymmetric with a tail extending to very large losses. This is illustrated by the measured data of Fig. 1. The distribution is expected to follow closely the shape calculated by Landau and Vavilov,[18] but modified by the possible escape of high energy knock-on electrons from the absorber. On the other hand, for heavy nuclei of charge Z, the average energy loss increases with Z^2 and will become as large or larger than the maximum energy of a single knock-on electron. In that case, the energy loss distribution will become very nearly Gaussian. As Fig. 8 shows, this is clearly the case for oxygen nuclei with $Z=8$. The absence of a high-energy tail in this distribution has the practical consequence that the superposition of a small transition radiation signal to the ionization loss measured in a MWPC, can be readily detected. Figure 9 shows how the width of the ionization loss distribution changes with increasing Z. The mean relative rms width varies, as expected, as $1/Z$, while the relative FWHM shows this $1/Z$ scaling only for higher charges, when the distributions are Gaussian.

The distribution of energy deposited by transition radiation can be estimated analytically by sampling the single-photon spectrum with a mean number of photons which scales as Z^2. We calculate the single-photon energy distribution for the fiber radiators by assuming they can be represented by an equivalent radiator of parallel foils with thicknesses and spacing given by the parameters of Table I. We then use a Monte Carlo method to estimate the total signal and its fluctuations for heavy nuclei traversing the MWPC together with transition radiation photons. The photon signals are added to a sample from the particle energy-loss distribution, which is observed directly at low energy. The sum represents a simulated signal in a MWPC from a heavy charged particle with transition radiation. Results of this procedure are shown in Fig. 8 with the calculated distributions at $\gamma = 4000$ for oxygen and iron. The *relative* rms widths of the calculated MWPC distributions do not change significantly with increasing energy, in fact they decrease slightly.

To compare this calculation with data from the space instrument, Fig. 10 shows relative rms deviation from the mean of the separate signals produced in the 6 MWPC's, for oxygen nuclei in two different energy ranges. This represents the fluctuation of the MWPC signals about the mean, for each event. The expected trend of these data, from calculations of distributions of the type shown in Fig. 8, is shown as a dashed curve. Note that we expect the relative fluctuations to decrease somewhat when transition radiation is produced (for $\gamma > 600$). These data indicate that the events with large mean pulse heights conform to the expected signal distributions in a single MWPC, and that they are not dominated by a large pulse height in one detector. We conclude that the combination of ionization loss and transition radiation from the high-energy nuclei have fluctuations in signal deposition that are close to the predicted distributions of Fig. 8.

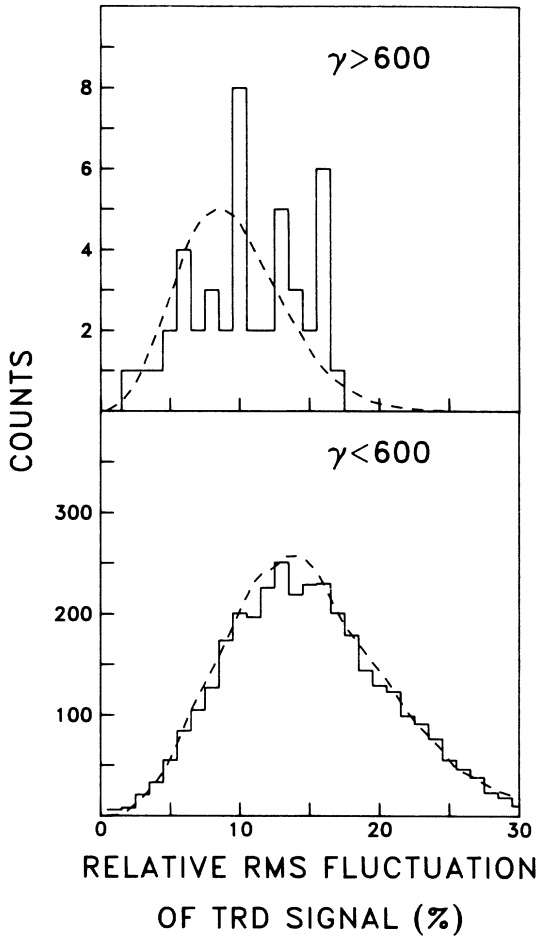

FIG. 10. Cosmic-ray oxygen event signals in the transition-radiation detector. A histogram of the relative rms deviation between the six multiwire chamber signals is plotted for two separate energy regions, $\gamma > 600$ and $\gamma < 600$. The dashed curves indicate expected distributions for $\gamma = 5$ and $\gamma = 4000$ based on the simulations of Fig. 8.

For a practical detector design two other effects which produce fluctuations are important. The first of these is the production of energetic knock-on electrons in the radiator material of the transition radiation detector, which can simulate x-ray photons by penetrating the MWPC. This could make a lower energy particle appear to have transition radiation. Since these knock-on electrons in general do not propagate close to the particle path, the effect can be suppressed by spatially segmenting the detector. A Monte Carlo model of this effect has shown that a spatial segmentation of the detectors into 5-cm strips as used in our experiment is adequate for this TRD.[19] For the stack of six independent chambers used

here the residual effect is negligible even for measurements of steeply falling cosmic-ray spectra where there are only a few high-energy particles.

A second effect that becomes important for high charges is that of limited streamer production.[20] A streamer discharge in the gas which produces a large pulse height in the MWPC, is formed when the collected charge exceeds a few pC. We have observed this effect at the Bevalac accelerator for heavy nuclei when the collected charge exceeded ≈ 10 pC. To ensure that all measurements in the TRD are in proportional regime, the gain of the MWPC's during the space flight was set at ≈ 20. At this level an iron nucleus produces ≈ 0.5 pC in the avalanche, well below the level at which streamers form.

From distributions similar to those of Fig. 8 the energy resolution of the TRD of the space instrument can be calculated. At $\gamma = 1000$ the rms energy resolution for oxygen and iron nuclei is 13% and 8%, respectively. The accuracy of the measurement for iron nuclei is dominated by the systematic fluctuations of the MWPC avalanche rather than by fluctuations in the energy deposited in the MWPC. A transition radiation detector therefore provides a good measurement of the particle energy for heavier nuclei. For measuring the steeply falling spectra of nuclei in the cosmic rays the absence of a significant tail of fluctuations to large pulse heights, makes the TRD particularly appropriate. With the space flight of our detector, we have determined the energy spectra of the major cosmic-ray nuclei with $Z > 4$ to energies above 1 TeV/nucleon. The upper energy limit of this measurement is determined by counting statistics due to the relatively short duration of the space flight rather than the dynamic range of the detector. The results of this measurement and a discussion of the astrophysical implications are published elsewhere.[7,16,22]

VI. CONCLUSIONS

We have detected the emission of transition radiation from relativistic nuclei in the cosmic radiation. The signal was observed in a multilayer TRD which was calibrated at an accelerator beam with singly charged particles. As expected, the response of this detector begins around $\gamma \approx 450$. Saturation of response was not seen up to the highest observed $\gamma = 3800$. Observations of high energy heavy nuclei in the cosmic radiation with a detector of this type has revealed no deviation of the mean signals observed in the MWPC from a simple Z^2 scaling law. A quantitative study of the fluctuations in the detected signals shows good agreement with the observed data. The transition radiation signal, relative to the background of ionization loss, exhibited only a weak dependence on the angle of entry of the particles, relative to a normal to the detector plane. Only at angles close to 60 deg. from the normal was an appreciable degradation in the relative transition radiation signal observed.

The application of this detector to the measurement of the energy of relativistic heavy nuclei is possible because the fluctuations in the observed signals are significantly below those due to singly charged particles. The fluctuations in the "background" ionization-loss signal are reduced partly by the increase in the number of Coulomb collisions, but also by the escape of high-energy knock-on electrons from the detector volume. The relative fluctuations in the transition-radiation component of the signal are reduced because of the large number of transition radiation photons produced by higher charged nuclei. In the region around 1 TeV/amu the detector described here has an energy resolution better than $\approx 15\%$ for nuclei with $Z > 4$. This technique is most appropriate for measurements of high-energy particles in the primary cosmic radiation with large area, low mass detectors.

ACKNOWLEDGMENTS

This work would not have been possible without the devoted efforts of the staff of our laboratory, in particular of L. Glennie, D. Bonasera, E. Drag, W. Harvey, W. Johnson, and R. Ray. We are also indebted to the staff of Fermilab, who helped us to perform the calibration measurements, in particular R. Dixon and G. Koizumi. This work was supported by NASA under Contract No. NAS 8-32828 and Grants Nos. NAGW-1311, NGL 14-001-005, and NGL 14-001-258.

---

*Also at Department of Physics, The University of Chicago, Chicago, IL 60637.

†Present address: California Institute of Technology, Pasadena, CA 91125.

[1]V. L. Ginzburg and I. M. Frank, Zh. Eksp. Teor. Fiz. **16**, 15 (1946); J. Phys. (USSR) **9**, 353 (1945).

[2]M. L. Ter-Mikaelian, *High Energy Electromagnetic Processes in Condensed Media* (Wiley, New York, 1972).

[3]V. L. Ginzburg and V. N. Tsytovich, Phys. Rep. **49**, 1 (1979).

[4]L. C. L. Yuan, C. L. Wang, and S. Prünster, Phys. Rev. Lett. **23**, 496 (1969).

[5]F. Harris *et al.*, Nucl. Instrum. Methods **107**, 413 (1973).

[6]M. L. Cherry, G. Hartmann, D. Müller, and T. A. Prince, Phys. Rev. D **10**, 3594 (1974).

[7]J. Grunsfeld, J. L'Heureux, P. Meyer, D. Müller, and S. Swordy, Astrophys. J. Lett. **327**, L31 (1988).

[8]See, e.g., the compilation of J. Linsley, in *18th International Cosmic Ray Conference, Bangalore, India, 1983, Conference Papers,* edited by N. Durgaprased *et al.* (TIFR, Bombay, 1983), Vol. 12, p. 135.

[9]M. L. Cherry and D. Müller, Phys. Rev. Lett. **38**, 5 (1977).

[10]M. L. Cherry, Phys. Rev. D **17**, 2245 (1978).

[11]S. P. Swordy, J. L'Heureux, D. Müller, and P. Meyer, Nucl. Instrum. Methods **193**, 591 (1982).

[12]J. H. Cobb, W. W. M. Allison, and J. N. Bunch, Nucl. Instrum. Methods **133**, 315 (1976).

[13]J. L'Heureux, J. Grunsfeld, P. Meyer, D. Müller, and S. P. Swordy, in *Proceedings of the 20th International Cosmic Ray Conference,* Moscow, USSR, 1987, edited by V. Kozyarivsky *et al.* (Nauka, Moscow, 1987), Vol. 2, p. 366.

[14]J. L'Heureux, J. Grunsfeld, P. Meyer, D. Müller, and S. P. Swordy, Nucl. Instrum. Methods (to be published).

[15]M. H. Salamon, S. P. Ahlen, and G. Tarlé, Phys. Rev. A **21**, 1506 (1979).

[16]J. E. Lamport, J. L'Heureux, P. Meyer, and D. Müller, in *16th International Cosmic Ray Conference, Kyoto, Japan, 1979, Conference Papers,* edited by S. Miyake *et al.* (Institute for Cosmic Ray Research, University of Tokyo, Tokyo, 1979), Vol. 11, p. 62.

[17]S. P. Swordy, D. Müller, P. Meyer, J. L'Heureux, and J. M. Grunsfeld, Astrophys. J. **349**, 625 (1990).

[18]L. Landau, J. Exp. Phys. (USSR) **8**, 201 (1944); P. V. Vavilov, Zh. Eksp. Teor. Fiz., **32**, 320 (1957) [Sov. Phys. JETP **5**, 749 (1957)].

[19]S. P. Swordy, D. Müller, and A. Ten-Have, in *18th International Cosmic Ray Conference, Bangalore, India, 1983, Conference Papers* (Ref. 8), Vol. 8, p. 55.

[20]S. Brehin *et al.*, Nucl. Instrum. Methods **123**, 225 (1975); M. Atac, A. V. Tollestrup, and D. Potter, *ibid.* **200**, 345 (1982).

[21]T. A. Prince, D. Müller, G. Hartmann, and M. L. Cherry, Nucl. Instrum. Methods **123**, 231 (1975).

[22]D. Müller *et al.* (unpublished).

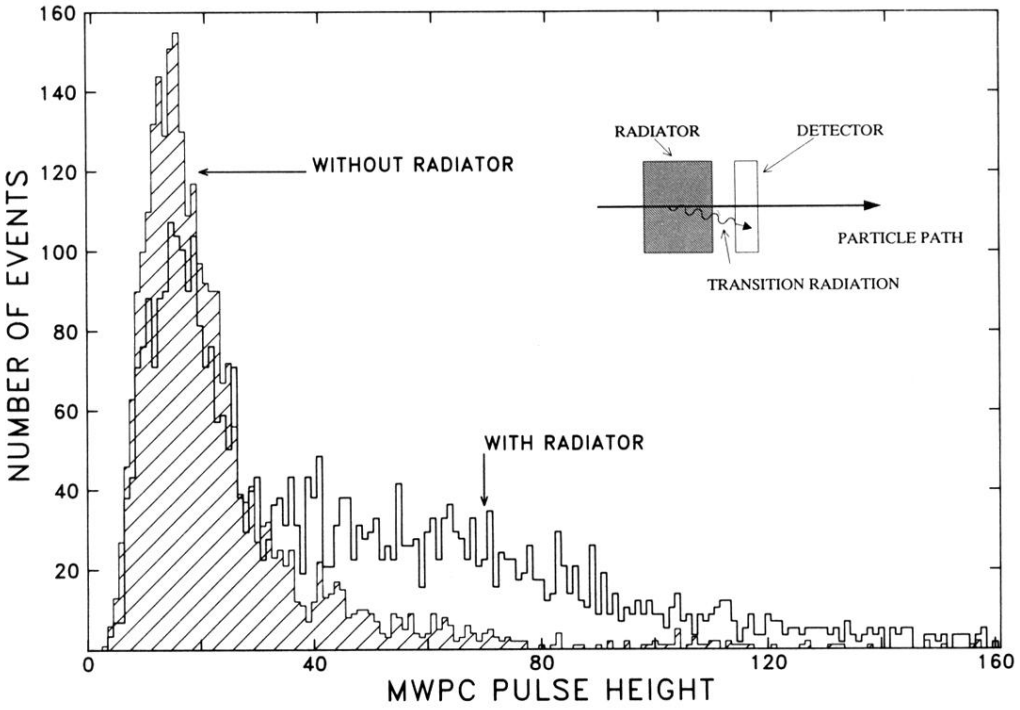

FIG. 1. The pulse-height distribution observed from a single multiwire proportional chamber in the transition detector for muons at 400 GeV/c. This includes the transition-radiation and ionization-loss components of the signal. The shaded distribution was obtained by replacing the radiator with an equivalent thickness of solid material, this gives only the ionization loss component of the signal. The inset shows the schematic arrangement of the detector.

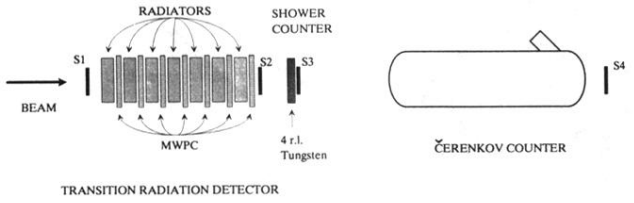

FIG. 2. Schematic of the experimental arrangement at Fermilab. The transition-radiation detector consists of six radiator–multiwire-proportional-chamber pairs. This experiment was used to determine the response of the detector for singly charged particles.

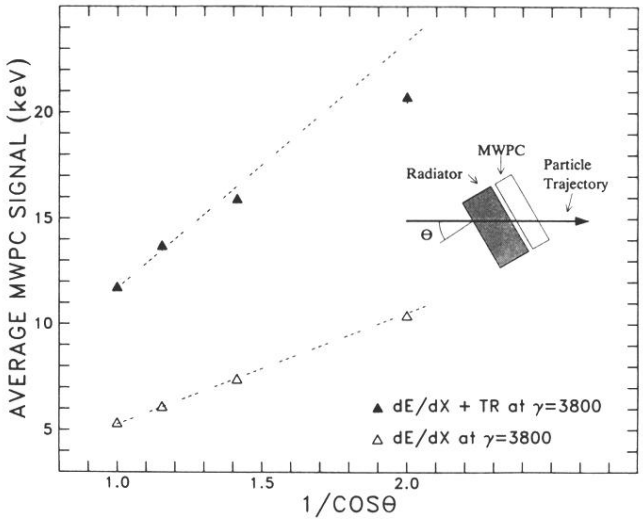

FIG. 4. The variation of the transition-radiation-detector response with incoming particle angle. At large angles the transition radiation component of the signal (upper points) begins to deviate from proportionality to $1/\cos\theta$ (upper dashed line). The ionization-loss signal, however, is strictly proportional to $1/\cos\theta$ (lower points).

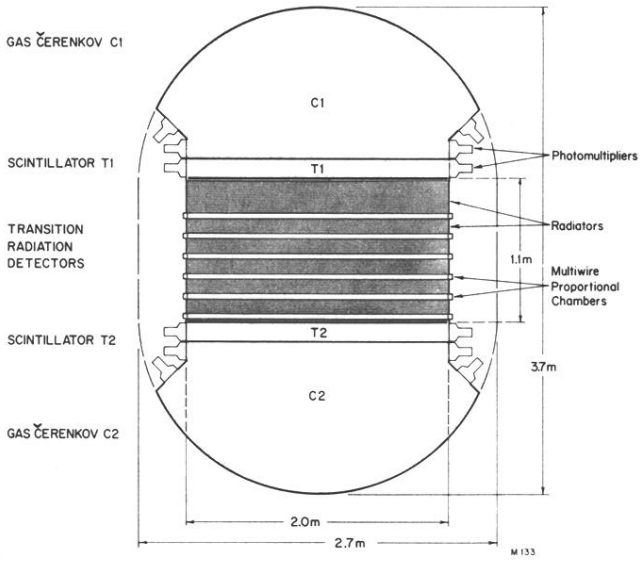

FIG. 6. Schematic cross section of the cosmic-ray instrument.

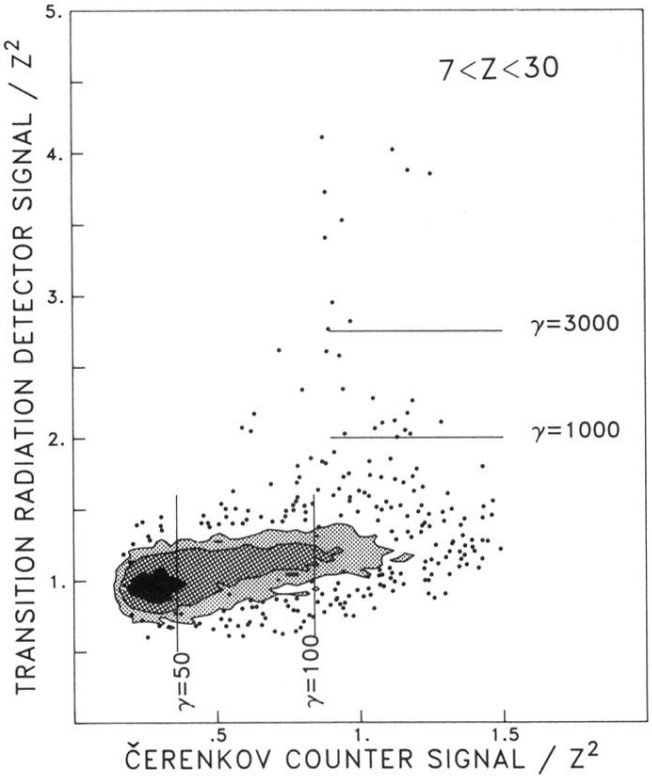

FIG. 7. Cosmic-ray nuclei event signals in the instrument for the range $7 < Z < 30$. For each event the transition radiation detector and Čerenkov signal divided by Z^2 are plotted. Examples of the energy calibrations are marked as lines for each counter. The contour levels are drawn where the event density is too large to distinguish individual points, each level represents a factor of 4 increase in event density. The area contained inside the lowest contour contains ≈ 9000 events. As expected, all the transition radiation events lie at the saturated level in the Čerenkov counter.